The Kondo Effect in an Artificial Quantum Dot Molecule

H. Jeong,[1] A. M. Chang,[1]* M. R. Melloch[2]

Double quantum dots provide an ideal model system for studying interactions between localized impurity spins. We report on the transport properties of a series-coupled double quantum dot as electrons are added one by one onto the dots. When the many-body molecular states are formed, we observe a splitting of the Kondo resonance peak in the differential conductance. This splitting reflects the energy difference between the bonding and antibonding states formed by the coherent superposition of the Kondo states of each dot. The occurrence of the Kondo resonance and its magnetic field dependence agree with a simple interpretation of the spin status of a double quantum dot.

The Kondo effect is a many-body phenomenon resulting from the spin interaction between localized magnetic impurities and conduction electrons. The recent discovery of the Kondo effect in artificial quantum dot systems (*1*–*7*) has raised much interest in the area of quantum impurity and the associated physics of electron spin and strong correlation. The Kondo problem in a quantum dot (*8*, *9*) is now well understood through experimental and theoretical studies. Further interesting physical situations can be found when we consider the interdot interaction in multiple quantum dots.

In a conventional metallic Kondo system with dilute magnetic impurities, the impurities are far apart and can be modeled by a single-impurity Anderson or Kondo Hamiltonian (*10*, *11*). The properties of such a system are well known where screening of an isolated impurity spin by the conduction electrons takes place. When the density of magnetic impurities is high, we can no longer ignore the spin-ordering tendencies due to interaction between impurities. The two competing effects that lead to two different tendencies of the system to interact with conduction electrons—the Kondo effect and the Ruderman-Kittel-Kasuya-Yoshida (RKKY) interaction (*12*–*14*)—have a crucial influence on the impurity magnetism. The conduction electron–mediated, RKKY indirect-exchange interaction favors magnetic ordering of impurities, whereas the Kondo effect tends to quench individual impurity spins. Theoretically the two-impurity Kondo problem provides a simple model to study these competing effects (*15*–*17*), and is important for the understanding of strongly correlated electrons. For example, Fermi and non-Fermi liquid behaviors, ferromagnetic and antiferromagnetic correlations, and diverse behavior of heavy fermion systems are all believed to result from the competition between Kondo and RKKY interaction.

The tunability of artificial quantum dots has brought unprecedented control to the investigation of the Kondo effect at the single-impurity level. It is a natural next step to inquire about the physics of interaction between multiple localized magnetic spin moments and conduction electrons in a double quantum dot system. Here, the impurities interact through an effective antiferromagnetic coupling, $J = 4\ t^2/U$, where t is the tunable interdot coupling and U is the intradot charging energy. These two new energy scales, t and J, are expected to introduce qualitatively new behavior. The rich physics of a double quantum dot Kondo system as a tunable, two-quantum impurity system has been studied extensively by theorists (*18*–*22*). More intriguingly, the double dot has recently been proposed as a feasible two-qubit system for quantum computation (*23*). Here, we report the observation of a coherent Kondo effect in a double quantum dot, which is a direct experimental realization of a two-impurity Kondo model.

Our device is fabricated on a GaAs/AlGaAs heterostructure (Fig. 1A). The sample is mounted in the mixing chamber of a dilution refrigerator parallel to the axis of a superconducting magnet. The lattice base temperature is 15 mK, whereas the electronic temperature is estimated at ~40 mK. It is possible to set each quantum dot to show similar characteristics by tuning gate voltages properly. Each dot exhibited two Kondo valleys represented by the pronounced zero bias maximum (ZBM) (Fig. 1B). We observe the Kondo ZBM only in the odd-electron Coulomb blockade (CB) valleys between CB peaks with a spacing smaller than that between the adjacent even-electron valleys. These Kondo valleys exhibit an increase in the conductance with decreasing temperature. ΔE and U were determined in the closed dot regime by the standard method of measuring the lever arm, α, and the differential conductance at finite source-drain bias to observe excited states. For the upper (lower dot), ΔE = 0.45 meV (0.37 meV) and the charging energy U = 1.92 meV (1.73 meV). These are comparable values reported previously by other groups for dots of similar size (*1*, *3*, *6*). To accomplish the delicate settings for forming the double dot, we used the gating information of each dot because all the gates are needed. For example, by using V1, V2, and V3, the upper dot is first formed. Next, V4 is biased up to the proper value; finally, V5 is energized. Because of mutual capacitive coupling, the center tunneling barrier becomes higher after energizing V4 and V2, and then needs to be reduced to maintain the optimum conduction characteristics through the center barrier.

Assuming simple, even-odd electron filling in each quantum dot, we can expect three unique spin configurations in a double dot. It is necessary to consider only the uppermost energy level in each dot because it is the most relevant one for Kondo physics (Fig. 1, C to E) (*24*). When both dots contain a single electron on their uppermost level, a coherent Kondo resonance can occur, which is the case that has attracted the most theoretical attention. If one or both of the dots contain a spin-singlet pair of electrons (Fig. 1, D or E), a coherent Kondo resonance cannot occur because Kondo coupling cannot be achieved throughout the double-dot system. In a series-coupled double dot, we can readily distinguish cases (C) and (D) because even if a Kondo resonance forms in (D) in one dot, transport is greatly impaired by the presence of the paired electrons in the remaining dot. Within this scenario, we expect a periodic occurrence of Kondo resonance (circled region of Fig. 2A) as electrons are added one by one.

To locate the valleys where a coherent Kondo resonance occurs, we first identified the valleys of relatively well-defined numbers of electrons in a manner analogous to the single dot case. In a two-dimensional plot of the double dot Coulomb blockade conductance peak position versus plunger gates, a honeycomb structure (Fig. 2A) is observed where the peak splitting depends on the coupling between the dots (*25*, *26*). The regions with a well-defined number of electrons can be found around the central region of each hexagon. It is necessary to follow and identify proper valley regions in every instance of pincher-gate voltage change, because a change in any pincher-gate V_1, V_3, or V_5 can produce a significant shift of the overall honeycomb pattern in

[1]Department of Physics, Purdue University, West Lafayette, IN 47907, USA. [2]School of Electrical and Computer Engineering, Purdue University, West Lafayette, IN 47907, USA.

*To whom correspondence should be addressed. E-mail: yingshe@physics.purdue.edu

the device. The most critical parameters in the experiment were the tunneling matrix between the dot and the leads, Γ, and the coupling strength between the two dots, t. The useful ranges of both Γ and t are constrained for the following reasons. Because the Kondo temperature, T_K, sensitively depends on Γ, then in order to maximize Γ and T_K, the dot-lead tunnel barriers need to be open enough to yield a conductance close to $2e^2/h$ (*1*–*3*, *5*). To optimize t, we note that if the dot-dot tunneling barrier is too high (small t), the overall conductance of the dot becomes small and the Kondo correlation becomes weak. On the other hand, if it is too low (large t), it is not possible to identify valley regions of hexagons, because the zigzag pattern of a double dot peak position approaches a set of parallel straight lines in the limit of perfect coupling. In the measured double dot conductance as a function of plunger gate voltages V2 and V4 (Fig. 2B), the center gate V3 is set such that it gives barely enough honeycomb structure for easy identification of the valley regions and also enough cotunneling conductance for the Kondo resonance. From the splitting of the Coulomb blockade peaks, we estimate an interdot conductance of ≈0.8 ($2e^2/h$) (*25*–*28*). In this strong tunneling regime, however, it is not straightforward to convert the conductance into a reliable estimate of t. To find out which valleys are Kondo valleys containing a single electron on each dot, we measured the differential conductance, dI/dV, versus voltage bias across the double dot in a total of 32 valley regions, four of which show zero-bias maximum peaks. For example, in the six numbered regions in Fig. 2B, we see the appearance and disappearance of zero-bias maximum Kondo resonance peaks roughly matched to Fig. 2A (Fig. 3).

Compared with the single dot case, the notable feature of the Kondo resonance peaks is its splitting into two peaks in zero magnetic field. Several theoretical papers have predicted that when the many-body molecular bonding and antibonding states are formed, the Kondo resonance shows a double peak structure in a coupled quantum dot (*19*, *20*, *22*). When the split peaks are symmetric (Fig. 3, valley 4), they are centered about zero bias, and for the nonsymmetric cases (Fig. 3, valleys 1, 3, and 6), the larger peak is closer to zero bias. We believe that the prevalence of the asymmetric situation is due to the difficulty in achieving the same condition on both dots. This is supported by the observation that for the symmetric trace 4, when either dot-lead tunnel barrier is changed through V1 or V5, we obtain a similar asymmetric double peak. Attempts to make asymmetrical peaks symmetric were less successful due to slight differences in the characteristics of the two dots and the mutual capacitance

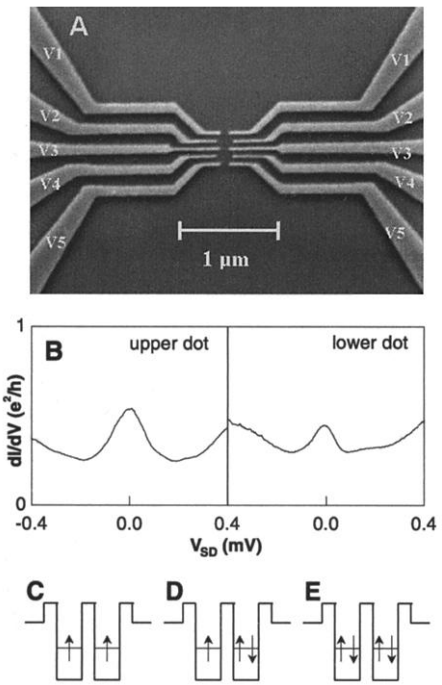

Fig. 1. (**A**) The dots are defined by 10 independently tunable gates on a GaAs/AlGaAs heterostructure containing a two-dimensional electron gas (2DEG) located 80 nm below the surface. The low-temperature sheet electron density and mobility are $n = 3.8 \times 10^{11}$ cm^{-2} and $\mu = 9 \times 10^5$/cm^2 Vs^{-1}, respectively. Lithographic dot size is 180 nm in diameter, and each dot contains about 40 electrons inside. To reduce an unnecessary degree of freedom in controlling the double dot, gates sitting on the opposite side are hooked together, giving a total of five pairs of controllable gates. Gate pairs V1 and V5 are used to set tunneling barriers, whereas V3 sets the interdot tunnel coupling between the dots. V2 and V4 control the number of electrons and energy levels in each dot separately. (**B**) Typical traces of Kondo resonance peaks when each dot is working as single dots. The upper dot shows larger Kondo resonance than the lower one. (**C** to **E**) Three unique cases of spin states of a double dot, based on a simple electron filling with spin degeneracy. (C) is the case that has been considered to show split Kondo resonance (*18*, *19*, *21*). (D) and (E) contain singlet electrons in one of the two dots, and the overall Kondo resonance is not allowed.

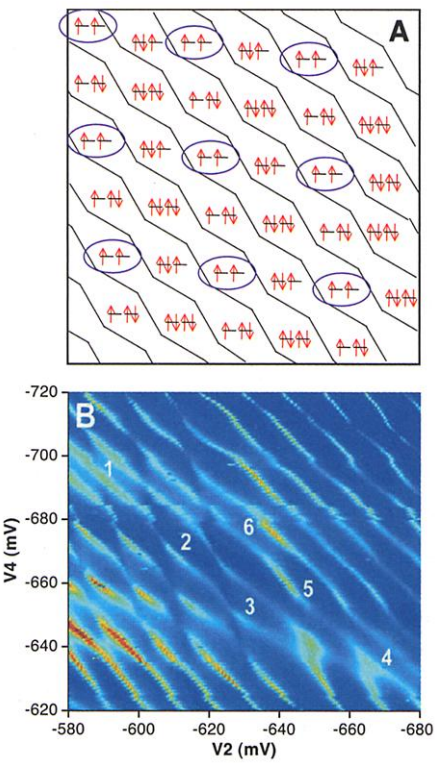

Fig. 2. (**A**) Schematic of a periodic structure of the electron spin configuration as a function of two gate voltages controlling the electron numbers in each dot in a double dot. The lines represent positions of Coulomb blockade peaks. This zig-zag pattern changes, depending on the interdot coupling strength controlled by V3. For simplicity, only the spins of last electronic levels are shown. Circled regions contain possible double–Kondo impurity spin status corresponding to the regions 1, 3, 4, and 6 in (B). (**B**) Color scale plot of the measured conductance of a double dot as a function of gate voltages V2 and V4. The center gate voltage V3 = −860 mV. Red (blue) color means higher (lower) conductance. The numbered valley regions, 1, 3, 4, and 6 show zero-bias maximum (see Fig. 3). Note that (A) is intended only as an illustration for comparison with (B). In a real device, the double dot characteristics gradually change as the plunger gate voltages are swept, and the honeycomb pattern inevitably appears distorted from the ideal situation.

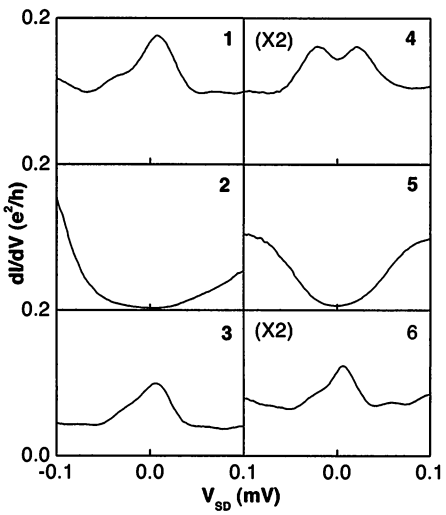

Fig. 3. Differential conductance traces from 1 to 6 in Fig. 2 B. Trace 4 and 6 are magnified by a factor of 2. The occurrence of Kondo resonance peaks is well contrasted. The periodicity is consistent with the diagram in Fig. 2A. A unique feature of the Kondo resonance peaks is their spitting, as compared with the single peaks from single dots (e.g., Fig. 1B).

and interdependence of the gates. In small devices such as ours, the gates are pushed closer together and experience stronger interdependence. The observed splitting $\delta \approx 45$ μeV is comparable to the molecular bonding-antibonding splitting of 10 to 120 μeV previously reported in double quantum dots (*29*, *30*). It is important to emphasize that our result demonstrates the formation of many-body bonding-antibonding Kondo states. Previous experiments were unable to determine the spin status of the double dots and were often configured to suppress Kondo correlation (small Γ), yielding a splitting that was single particle in nature. The height of split peaks is about an order of magnitude smaller than that of single dot Kondo resonance peaks, perhaps because the double dot is more resistive or because of antiferromagnetic coupling between the single localized electrons in the two dots. For sufficiently large antiferromagnetic coupling, the Kondo effect will be suppressed because it is more favorable for the localized spins to form a spin singlet than to form a Kondo singlet with conduction electrons. The gap between double peaks can be adjusted to a certain extent (Fig. 4A), depending on the gate voltage settings—for example, by changing the coupling of two dots or coupling of the dots to the leads. However, we were unable to observe single peaks in the regime where the dot-dot coupling is smaller than the dot-lead coupling mentioned in theories. In the case where the coupling of two dots is reduced, the decrease in overall conductance was too large in this series-coupled configuration, and a clear signature of zero-bias maximum was no longer observable.

All four split Kondo peaks showed qualitatively similar results in magnetic and temperature dependence. The parallel magnetic field dependence (Fig. 4B) of the symmetric peak trace 4 in Fig. 3 shows that as the magnetic field increases, the two split peaks approach each other, merge, and then split again. When the magnetic field is applied, the Zeeman effect splits the two many-body molecular states formed around the Fermi levels, giving a total of four peaks. Two of the four peaks closest to the midpoint of the left and right Fermi levels overlap when the source-drain bias, V_{SD}, is applied, cross, and split again. The contribution from the other two outside peaks should, in principle, be present but is not observed, possibly because of spin decoherence at larger bias. Similar behavior is also present in the single-particle, two-level Kondo system (*4*, *7*) where only two out of four peaks are clearly visible. We can estimate a rough value for the electron magnetic moment g factor on the basis of the Zeeman energy. We find a value of between 0.3 and 0.6 compared with the known magnitude of 0.44. As the temperature increases, both of the split peaks tend to decrease and finally disappear (Fig. 4C). In this temperature dependence, the zero-bias conductance of the symmetrically split peaks increases slightly at first, and then decreases as the temperature increases (Fig. 4D). Even the double peak structure disappears; the overall broad peak is maintained in the higher temperature range. This may indicate the effect of the antiferromagnetic spin coupling competing with the Kondo correlation. If the energy scale of antiferromagnetic coupling is smaller than the Kondo temperature, it will be destroyed faster than the Kondo resonance. Because the antiferromagnetic coupling reduces the conductance (weaker Kondo coupling), this overall feature will show a conductance maximum in temperature dependence. On the basis of the saturation temperature of the zero-bias peak height, the Kondo temperature is ~500 mK.

From our study, we find that the spin status of multiple dots is consistent with an interpretation based on electron spin filling in a double quantum dot. The Kondo resonance peaks in this system showed clear splitting as an indication of the Kondo effect in a quantum dot molecule. A more quantitative analysis of the competition of Kondo singlet energy versus antiferromagnetic coupling energy in a tunable manner with the advancement of quantum dot device technology will elucidate diverse physical phenomena in multiple quantum dot systems.

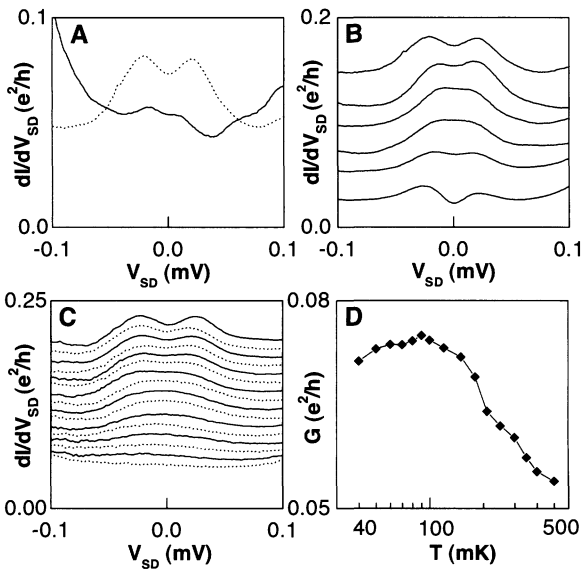

Fig. 4. (**A**) Peak splitting changes depending on the coupling of the two dots. Dotted (solid) line is for V3 = −860 mV (−870 mV). The solid line is magnified by a factor of 2. For each case, the splitting is 42 μV and 26 μV. (**B**) Magnetic field dependence of the symmetric Kondo resonance peak 4. Traces are measured at 0, 0.25, 0.5, 0.75, 1.0, and 1.25 T. The curves are offset by 0.02 e^2/h for clarity. Other peaks also show qualitatively similar behavior. The Zeeman splitting from two split peaks enhances the conductance at zero bias as the field increases because of the overlap of the density of states from the two peaks. At higher fields, they split further apart, as in the case of a single resonance peak. (**C**) Temperature dependence of differential conductance. From top to bottom: T = 40, 50, 60, 70, 80, 90, 100, 120, 150, 180, 210, 250, 300, 350, 400, and 500 mK, offset by 0.01 e^2/h for each line. The overall conductance structure decreases as the temperature increases. (**D**) Conductance at zero bias; the temperature T is shown on a logarithmic scale. Increasing the T causes the conductance to increase initially and then decrease.

References and Notes

1. D. Goldhaber-Gordon *et al.*, *Nature* **391**, 156 (1998).
2. S. M. Cronenwett, T. H. Oosterkamp, L. P. Kouwenhoven, *Science* **281**, 540 (1998).
3. J. Schmid, J. Weis, K. Eberl, K. v. Klitzing, *Physica B* **256**, 182 (1998).
4. S. Sasaki *et al.*, *Nature* **405**, 764 (2000).
5. W. G. van der Wiel *et al.*, *Science* **289**, 2105 (2000).
6. Y. Ji, M. Heiblum, D. Sprinzak, D. Mahalu, H. Shtrikman, *Science* **290**, 779 (2000).
7. J. Nygard, D. Henry Cobden, P. E. Lindelof, *Nature* **408**, 342 (2000).
8. L. I. Glazman, M. E. Raikh, *JETP Lett.* **47**, 452 (1988).
9. T. K. Ng, P. A. Lee, *Phys. Rev. Lett.* **61**, 1768 (1988).
10. J. Kondo, *Prog. Theor. Phys.* **32**, 37 (1964).
11. P. W. Anderson, *Phys. Rev.* **124**, 41 (1961).
12. M. A. Ruderman, C. Kittel, *Phys. Rev.* **96**, 99 (1954).
13. T. Kasuya, *Prog. Theor. Phys.* **16**, 45 (1956).
14. K. Yosida, *Phys. Rev.* **106**, 893 (1957).
15. C. Jayaprakash, R. Krishnamurthy, J. W. Wilkins, *Phys. Rev. Lett.* **47**, 737 (1981).
16. B. A. Jones, C. M. Varma, *Phys. Rev. Lett.* **58**, 843 (1987).
17. ———, J. W. Wilkins, *Phys. Rev. Lett.* **61**, 125 (1988).
18. A. Georges, Y. Meir, *Phys. Rev. Lett.* **82**, 3508 (1999).
19. R. Aguado, D. C. Langreth, *Phys. Rev. Lett.* **85**, 1946 (2000).
20. C. A. Büsser, E. V. Anda, A. L Lima, M. A. Davidovich, G. Chiappe, *Phys. Rev. B* **62**, 9907 (2000).
21. W. Izumida, O. Sakai, *Phys. Rev. B* **62**, 10260 (2000).
22. T. Aono, M. Eto, *Phys. Rev. B* **63**, 125327 (2001).
23. D. Loss, D. P. DiVincenzo, *Phys. Rev. A* **57**, 120 (1998).
24. Note that in Figs. 1C and 2A, a single upward-pointing arrow denotes an unpaired electron. It is not intended to represent the actual direction of spin alignment. In fact, in a complex many-body state, the dot spin most likely contains projections from both up and down spin states.
25. F. R. Waugh *et al.*, *Phys. Rev. Lett.* **75**, 705 (1995).
26. C. Livermore, C. H. Crouch, R. M. Westervelt, K. L. Campman, A. C. Gossard, *Science* **274**, 1332 (1996).
27. K. A. Matveev, L. I. Glazman, H. U. Baranger, *Phys. Rev.* B **53**, 1034 (1996).
28. J. M. Golden, B. I. Halperin, *Phys. Rev. B* **53**, 3893 (1996).
29. R. H. Blick, D. Pfannkuche, R. J. Haug, K. v. Klitzing, K. Eberl, *Phys. Rev. Lett.* **80**, 4032 (1998).
30. T. H. Oosterkamp *et al.*, *Nature* **395**, 873 (1998).

31. We acknowledge S. Hong for indispensable help in software development. Supported by NSF grant DMR-9801760.

6 June 2001; accepted 14 August 2001